Benlefki, Abdelkrim; Douaiba, Benouada; Abbes, Azzi

A SEA BREEZE NUMERICAL SIMULATION AND CIRCULATION ANALYSIS IN ORAN, ALGERIA, URBAN ATMOSPHERE

A SEA BREEZE NUMERICAL SIMULATION AND CIRCULATION ANALYSIS IN ORAN, ALGERIA, URBAN ATMOSPHERE

Abdelkrim Benlefki[*], Benouada Douaiba and Azzi Abbes

Faculté de Génie Mécanique, l'Université des Sciences et de la Technologie d'Oran, Algaria.

Abstract: In this paper the sea breeze dynamics in Oran agglomeration atmosphere, in the north Algeria, is investigated and analyzed by a numerical simulation of Oran agglomeration atmosphere, using SUBMESO model during diurnal cycle of June 24, 2010, in order to predict the spatio-temporal starting of sea breeze, its intensity and relative direction through atmospheric flow variations analysis, and to evaluate the role of thermal circulations on sea breeze direction, intensity and ventilation and its effect on pollutant transport. The study of this area has not been investigated or analyzed in any framework, the numerical simulation was preceded by a topographic and surface data processing in order to generate the grid simulation, with a specific characteristics used by the SUBEMESO and SM2-U (Soil Model for Sub-Meso scales Urbanized) models. This simulation allowed us to know all sea breeze characteristics during the study period.

Keywords: Urban Atmosphere; Sea Breeze; Meso scale Model; Soil model

---

[*] Correspondence to: Abdelkrim Benlefki. E-mail: abdelkrim.benlefki@gmail.com

INTRODUCTION

From the physical viewpoint, an environmental area is seen as a set of non-natural materials, which have different radiant and thermal properties from the vegetation cover. Its morphological structure depends on the irregular arrangement ground deformation of different sizes, more or less spaced between them. This arrangement will change the value of the aerodynamic roughness. Moreover the presence of residual vegetation and bare soil is also a feature of the agglomeration. The atmospheric zone is directly influenced by the presence of this agglomeration. Its scale is characterized by sub-meso scale to meso scale, around 10 km to 100 km. The urban area atmosphere studies are very complex and relatively recent. This atmosphere is the place of interaction between many dynamic, thermal and radiant mechanisms. The studies of the dynamics atmosphere are possible with the help of numerical simulations because experimental studies are very difficult, and numerical simulations allow having a resolution in four dimensions.

This work presents the dynamic sea breeze numerical simulation over Oran agglomeration, which is the area grid domain, with the SUBMESO model. The aerodynamic and thermodynamic processes at the interface between the surface and the atmosphere will be calculated using the soil model (SM2-U) directly coupled to the principal model.

THE SEA BREEZE

The heat contrast between the sea and the ground surfaces results a gradient of temperature between the air above the land and the air above the sea. The land and sea surface have different properties and energy balances. The land has a very small thermal conductivity and so heats and cools rapidly, resulting in a marked diurnal variation (Abbs, 1992). Conversely, the sea is a fluid in continual motion, any heating or cooling is distributed to a considerable depth and so the rise or fall of water surface temperature is only slight. This results in a very small diurnal variation in sea surface temperature.

A pressure difference at low levels in the atmosphere is produced due to the land-sea temperature difference increasing during the day, which results in the development of the sea breeze circulation (Simpson, 1994). The onshore flow blowing across the coast is known as the sea breeze. The sea breeze circulation (Finkele, 1995) cell begins near the coast in the morning and expands both landward and seaward (Corpetti, 2010), the overall pressure gradient is steady from day to day, the arrival of the sea breeze can be expected regularly every day at the same time, reaching strength of 6 or 7m/s (Simpson, 1994). The most of the existing studies are based on satellite images (**Fig. 1**) (Corpetti *et al.,* 2010) and have been performed manually in the form of experimental studies and observations (Cheng, 2002; Bastin *et al.*, 2005; Bouchlaghem *et al.*, 2007; Muppa *et al.*, 2012; Marvakou *et al.*, 2012), and the numerical studies have used regional scales models such as RAMS, MM5 and CAMx (Ding et al., 2011; Lee *et al.*, 2011); no automatic method is able to detect the sea breeze and analyze its behavior at meso and sub-meso scales, which are finer scales. In Damato *et al.*, 2003, for instance, the authors have manually extracted the sea breeze front once a day (at the warmest period) and have analyzed its behavior and the importance of its inland penetration (Stephan, 1999). Why this work going to help in studies of the sea breeze by a numerical approach with scales smaller for more precision.

SIMULATION DOMAIN AND MESH GENE-RATION

The simulation domain

The overall study area domain is about 1700 km² of which more than 40% is a liquid surface (Mediterranean Sea and Oran's Lakes), starting from the west coast of Oran (EL AOUNE) west to the western city of Arzew and from Oran's Sabkha in the south to some kilometers in the Mediterranean Sea in the north of Oran city (**Fig. 2**).
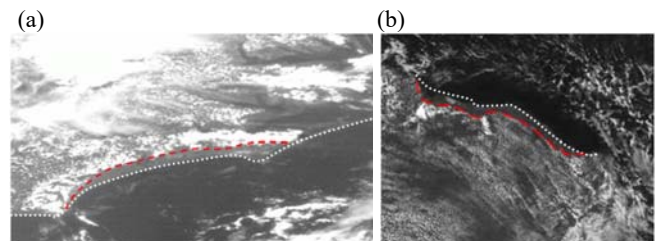

Fig.1 Sea breeze satellite image visualization the white line corresponds to the coast line whereas the red line corresponds to the sea breeze front. (a) Brazilian coast, (b) England coast (Corpetti *et al.*, 2010).
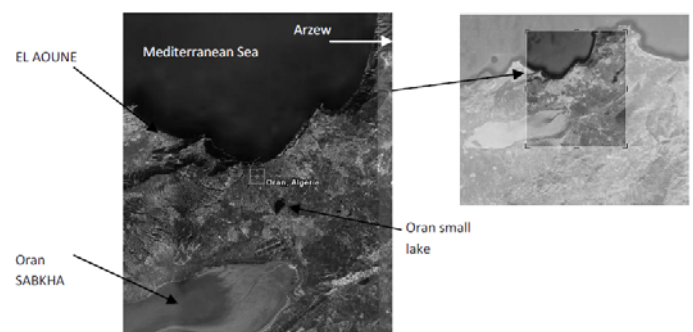

Fig. 2 Computing domain satellite image.

The data files are exactly those of the topography of Oran agglomeration, an area of about 40 km in the X direction approximately 0°47′2″W to 0°21′18″W, and about 43 km in the Y direction approximately 35°31′16″N to 35°52′52″N, with a step (Δx = Δy) of 990 m in both directions.

The topography

The topography data were retrieved from NOAA (National Oceanic and Atmospheric Administration), with Global relief model (ETOPO1) using NGDC's (National Geophysics Data Center) grid translator, with geographical form, i.e. with the coordinates (latitude, longitude, altitude), but the mesh should be in the Cartesian coordinates as it is a Gel-Chen type, characterized by a followed lower limit (topography) and a vertical stretch, (Nils 2003), composed of hexa cells, so the coordinates are transformed and classified according the Cartesian axis of the system (X, Y, Z). **Figure 3** shows the numerical representation of the domain's topography field and **Fig. 4** shows a three dimension view of the domain with surface deformation.

Tiny structures classification

Layout and fonts for the front matters

Follow the format presented in the print sample for the front matter and the instructions in this chapter. As the SUBMESO model used in this study is directly coupled with a soil model (SM2-U), (Leroye, 2003; Dupont, Mestayer, 2006**)**, a classification of the tiny structures of the entire ground surface area, a partial search has been made to this classification according to type of land of Oran agglomeration.

On the Oran town and all Oran entire regions there are three main types of natural sol types, bare soil which represents the smallest portion, the vegetation that focuses on the most of the mountains with a high
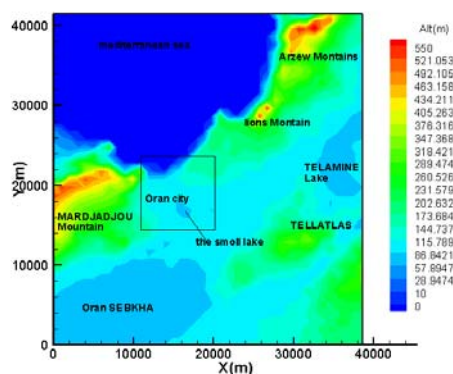

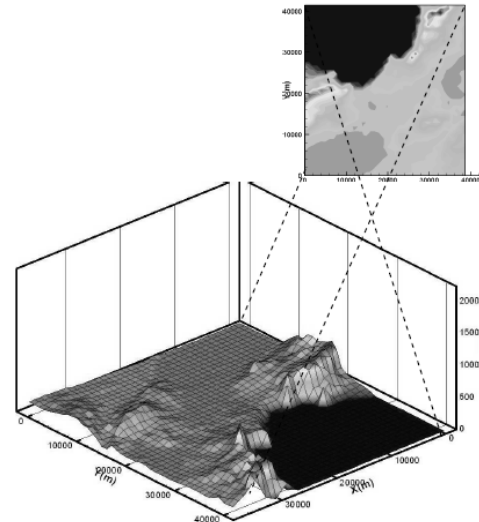**Fig. 3** Oran agglomeration topographic field.

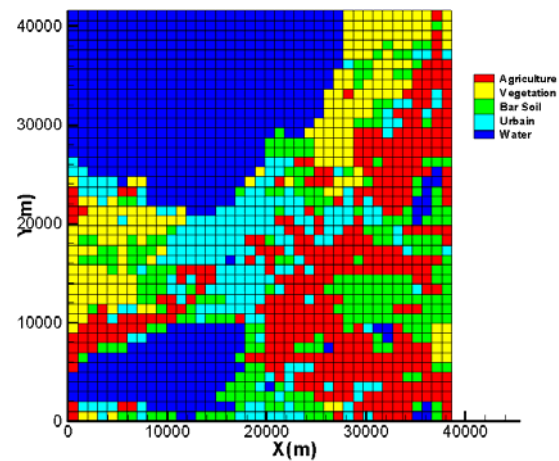**Fig. 4** Three dimension view of Oran agglomeration topography.

Fig. 5 Simulation domain soil types.

percentage and agriculture which is located on the southern area, the only non-natural class is a urbanized area, that represents the city of Oran, communes and villages in the Oran Wilaya (**Fig. 5**).

The simulation mesh

The topography used is from the(National Geophysical Data Centre (NOAA). It is available at 1km ± 10m resolution on all the area. The increase of the thickness of the mesh on the vertical axis above the topography is performed using the mesh by obeying geometric sequences (**Fig. 6**). Three steps are considered.

- Geometric sequence with it first value is 15m and the progressing factor of 1.12 is applied to 8th level (i.e. ≈ 151m above the first topographic level).
- Geometric sequence of 1.13 achieves the same altitude for all points on the 30th level, 4000 m above sea level.

- The last levels are progressing very close to 1.0001 due to the top of a field so a height of 9600 m above sea level.

The **Table 1** show the mesh resolution With Δx is the step in the X direction, Δy is the step in the Y direction, n_x is number of cells in the X direction, n_y is number of cells in the Y direction, n_z is number of cells in the X direction, Z_{min} is the height of the first mesh and Z_{avr} is the average of Δz.

Table 1. Oran agglomeration mesh resolution

$\Delta x = \Delta y$	n_x	n_y	n_z	$Z_{min}(m)$	$Z_{avr}(m)$
990	41	44	41	15	221

Boundary conditions and day choice

For the bottom the turbulent flux at the surface are calculated with the soil model SM2-U, which can be taken as constant (Dupon *et al.*, 2006; Dupont, 2006). For the lateral boundaries the SUBMESO model uses the external forcing and in the top of the domain the Rayleigh zone is applied when θ and $w \rightarrow 0$ and u, v and $q \rightarrow$ initial value. June 24 2010 was chosen for this study because it is totally sunny day which is a fully clear sky according to the National Office of Meteorology of Oran, Algeria, ONMO (*l'Office National de Météorologie d'Oran*), this feature allowed us to consider that the solar radiation is total then no obstacle between the sun and the surface, (all cloud's types).

The main data for the external forcing has been recovered from the Institute of Hydrometeorology of Formation and Research Oran, IHFR (*l'Institut de Hydrométéorologie de Formation et de Recherche*) for the four grid sides, which are treated according to the resolution of the simulation grid.

SIMULATION MODEL AND MODELING

The SUBMESO model

Atmospheric flows as any other academic and industrial flow are described by momentum equations (Navier-stokes), which are non-linear equations based on the theories of classical physics which express the laws of conservation. The equation of state which reflects the local balance of fluid and that of continuity describe the mass conservation, the equation of energy balance describes its conservation.

The Navier-Stokes equations are solved in compressible formulation, which is presented by air density variation (d$\rho \neq 0$), the non-hydrostatic which introduces the non-linear change of pressure in terms of altitude (z), in order to describe the evolution of prognostic variables from an initial state. The resolution of these equations is in a turbulent regime; therefore the flow's characteristics vary rapidly in time and in space, then a large degree of freedom is involved in the solution. When working with the meso scale or sub-meso scale, the vertical acceleration is not negligible.

In the model and only the pressure (p), specific humidity (q) and potential temperature (θ), a simplification is used in such a way that each variable is written as follows:

$$\phi = \underbrace{\overline{\phi}}_{\substack{\text{Basic} \\ \text{stat}}} + \underbrace{\phi'}_{\text{perturbation}} \qquad \phi = p, \rho \;\; \text{or} \;\; \theta \qquad (1)$$

The soil model

The Soil Model for sub-Meso scales urbanized version (SM2-U). This single canopy later model is a force-restore type model built on a physical form the ISBA rural soil model of (Noilhan, 1989) by including urban surface to surfaces to evaluate the heat and humidity fluxes at the urban canopy-atmosphere interface and then provide the lower boundary condition of the computational domain in simulation of the urban boundary layer. SM2-U has the advantage to be a unique model converting both rural and urban soils. Furthermore the physical processes inside the canopy, such as heat exchanges, heat storage, radiative trapping, water interception or surface water runoff, are integrated in a simple way.

SM2-U keeps the principal characteristics of the force-restore model (Dupont and Mestayer, 2006; Dupont *et al.*, 2006). The surface dynamic influence is represented through roughness lengths and displacement heights. The horizontal exchanges inside the canopy are not considered except radiation reflections and water runoff from saturated surfaces. The wind advection between urban surfaces is neither considered.
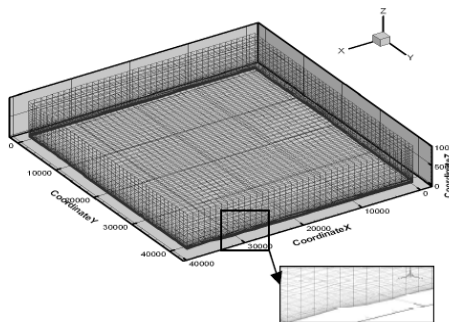

Fig. 6 The 3D grid simulation with the zoo of the first levels.

RESULTS AND DISCUSSION

In the present work the large eddy simulation is used by the SUBMESO model, accordingly to this so the results are in instantaneous values, the model running is followed by a statistical treatment in order to visualize the results, why the results are averaged over 1 hour.

The aim of the simulation is to analyze the sea breeze behavior over Oran agglomeration during the period in question, according to sea breeze definition and to better detect the phenomenon, as the sea breeze flows at low altitude and view to its relation to the temperature of the air above the ground surface, the best configuration is to present the horizontal velocity vectors with the potential temperature field at the first level of the mesh (**Fig. 7**).

At the beginning of the simulation duration that represents the real time, in the first two hour the dynamics of the atmosphere above the area is almost stationary, so there is not a change in either direction or in the intensity of the main flow, in **Fig.7 (a)**, after two hours (2.0 UTC) the main flow is generally from the south-west of the city of Oran and it is diverted to various direction by the Mardjadjou mountain range and Lions mountain, the wind is channeled between these two chains passing over the Oran city to the Mediterranean sea. The wind join a small mass of air arriving from the north-west over the sea, the two winds create turbulence at few kilometers from the coast. All on a low gradient potential temperature field, with average value of 296 K. During this time the sea breeze is absent.

The wind dynamics at 3.0 UTC (**Fig. 7b**) It appears broad from the Oran coast a flow of a strictly westbound with a synoptic wind that dominates the whole area it's come from the south west. After one hour, at 4.0 UTC (Fig.7 c) we can see a small increase in the temperature of the air layer adjacent to the surface, but this increase is insufficient to influence the flow dynamics, and the sea breeze is still absent.

Between 4.0 UTC and 5.0 UTC (**Fig.7 d**), the temperature increases remarkably mainly on the east side and south-east, this warming is due in fist part to the mass of hot air that comes from the south and secondly to soil warming by solar radiation as the sunrise that day is within this range of time. The south wind is warm because it comes from the inner region of western Algeria, which is not far from the northern Algerian Sahara, this wind is characterized by a high temperature at night, and given that sun begins to appear that day at about 5:40 min on the Oran region its radiation participates in the heating of the soil and consequently the air that is above, having regard to the dynamic wind that comes from the sea to the Arzew city in the extreme east of Oran (**Fig7. d**), channeled between Lions Mountains and Arzew mountains,

carrying with it a cold mass is noted, it'll cool while his traffic lane, this circulation traffic is not considered as a sea breeze because the wind direction results from the interaction between the two winds from the beginning of the day, the rest of the field there is not a change in the dynamics of the atmosphere.
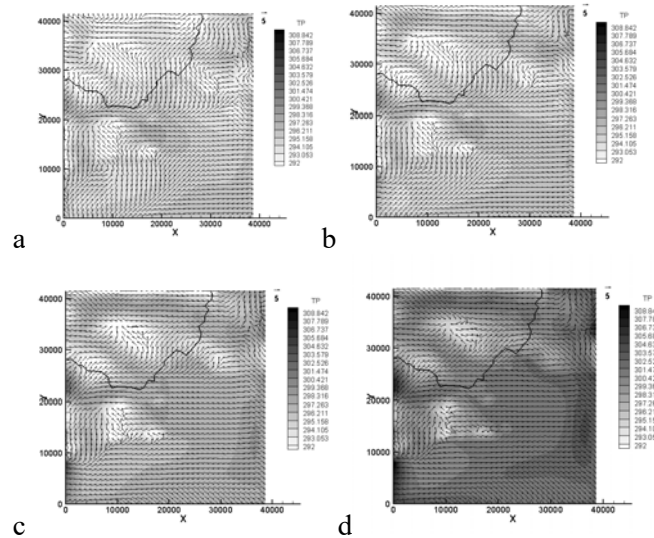

Fig. 7 Potential temperature field (in Kelvin) and horizontal section at the first SUBMESO model level (z = 7.5m), with the horizontal wind velocity (m/s) vector and the cost line, with black line corresponds to coast line, (a) at 1.0 UTC, (b) at 2.0 UTC, (c) at 3.0 UTC, (b) at 4.0 UTC.

Up to 6.0 UTC (**Fig. 8a**) the dynamics of the atmosphere does not change very remarkably from previous hours as there is no significant change of the dynamic or thermal parameters on the most part of the domain.

At 7.0 UTC (**Fig. 8b**), the temperature gradient between the air above the sea and over the land become more at least important, it attains 12 K, the maximum temperature of air above the soil touches 304 K, this value is due to the warming of the soil by sun radiation which become more intense at this time, this temperature gradient results an circumvention of the wind a few kilometers (northern area) above the sea to the land, at this hour we can say that the sea breeze starts triggered at a small scale, mainly on the part between Oran and Lions mountains with a velocity of 5m/s.

At 8.0 UTC (**Fig. 8c**), the mass of hot air that came from the south disappear because it is replaced by a wind that come from the north-west over the coast of the Oran city from LAEOUNE until Arzew mountains, it is the sea breeze, it penetrates to the southeast through the Oran small lake and Telatlas and Oran Sabkha after deflected by the mountains of Mardjadjou with a velocity increases to 6m/s proportionally to the temperature gradient that increases compared to the preceding hours.
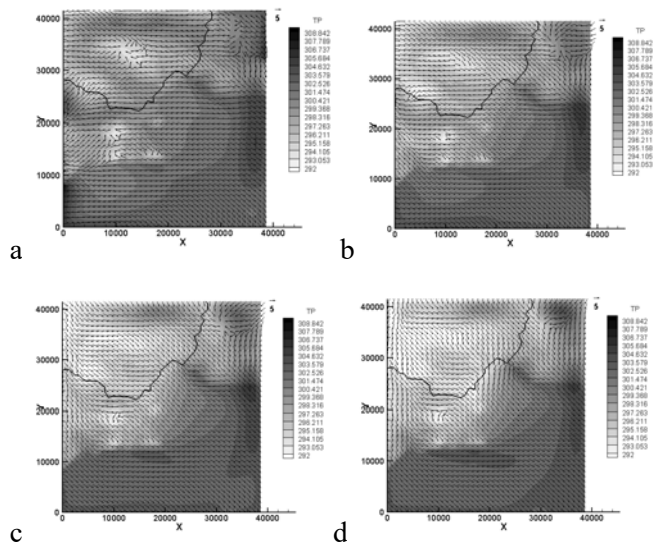
Fig. 8 Potential temperature field (in Kelvin) and horizontal section at the first SUBMESO model level (z = 7.5m), with the horizontal wind velocity (m/s) vector and the cost line, with black line corresponds to coast line, (a) at 6.0 UTC, (b) at 7.0 UTC, (c) at 8.0 UTC, (b) at 9.0 UTC.

From 9.0 UTC (**Fig. 8d**) to 13.0 UTC (**Fig. 9a**), the sea breeze remains dominant throughout the Oran agglomeration, with a slight speed increase by 7% as the temperature gradient between the land and sea become gradually more important because the sun is at the zenith, the potential temperature be at a maximum value of 305K on the east of the city of Oran and about 299K on the city, the direction of the sea breeze changes gradually to a strictly north, the sea breeze carries with it a cold air mass which drop the temperature of the atmosphere throughout the coast of Oran golf, over the city and some kilometers inland, the area of Lions Mountain is not cooled as the breeze is lifted behind the mountain, the vertical velocity component take a new direction with more or less important value, a recirculation is noticed after the mountains (**Fig. 12**), this recirculation prevents the detained air to be cooled, similar to flow over a the hill (Castagna, 2014; Chaouat, 2013; Prospathopoulos, 2012; Guangbiao, 2012; Jia-mei 201; Griffiths, 2010; Loureiro, 2008; Tessiani, 2007; Uchida, 1997).

At 15.0 UTC (**Fig.10 a**), the dynamic situation is practically unchanged compared to noon, except that low-wind begins to penetrate from the east but this happiness does no influence on the rest of the field. At 18.0 UTC (**Fig. 10 c**) through 16.0 UTC (**Fig. 10 b**) the wind comes from the east become more intense and it carries with it a cold mass will erase the stored heat near the surface and behind the Lions mountains, this wind will also meet the sea breeze with its northbound wind they create disturbances in the center of the field, the perturbation is amplified by the obstacles (mountains
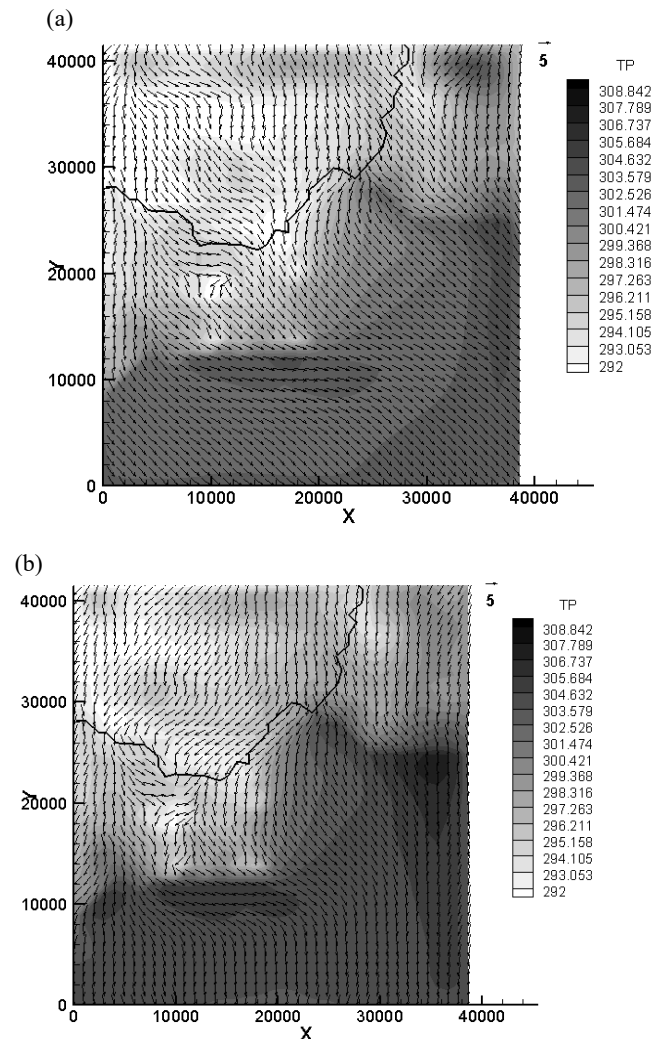
(a)

(b)

Fig. 9 Potential temperature field (in Kelvin) and horizontal section at the first SUBMESO model level (z = 7.5m), with the horizontal wind velocity (m/s) vector and the cost line, with black line corresponds to coast line, (a) at 13.0 UTC, (b) at 14.0 UTC.

and the city) and the rate of heat transfer increases which results in a remarkable cooling with an its distribution near to homogeneity, cooling is also due to the fort sun declination to the west and toward the sunset time. At 20.0 UTC (**Fig. 10 c**) the recirculation of the atmospheric flow and turbulent forms cause a new distribution of potential temperature which is not too heterogeneous on all the domain with a relatively low temperature gradient and a temperature value in the limit of the previous hours, it has not diminished because of heat stored in the ground which is due to the physical properties different to those of the sea, the new distribution of temperature directly affects the behavior of the breeze where it's braked and deflected by turbulent forms, from this moment the sea breeze starts of being weak and back in form and intensity.
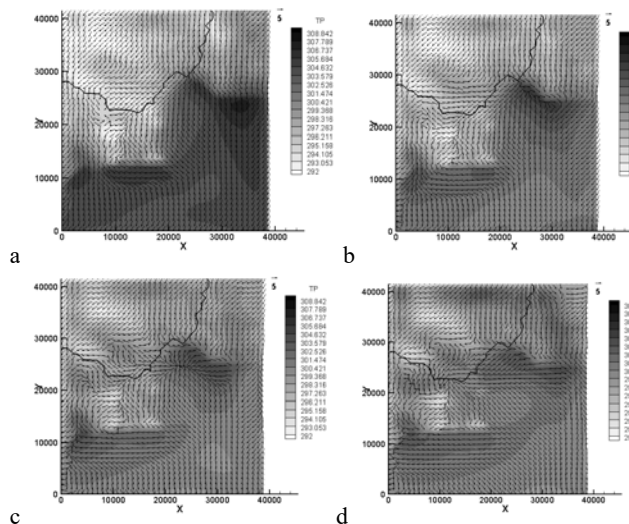
Fig. 10 Potential temperature field (in Kelvin) and horizontal section at the first SUBMESO model level (z = 7.5m), with the horizontal wind velocity (m/s) vector and the cost line, with black line corresponds to coast line, (a) at 15.0 UTC, (b) at 16.0 UTC, (c) at 18.0 UTC, (d) at 20.0 UTC.

At the end of the day and, after the sunset (**Fig. 11 a**, **Fig. 11 b**) the temperature of the air on the whole Oran agglomeration and also the temperature gradient decreases which result the disappearance of the sea breeze, an east wind replaces the breeze.
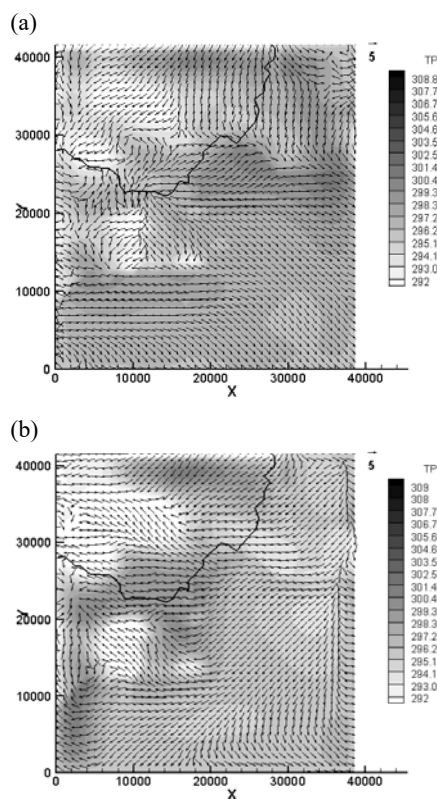

Fig.11 Potential temperature field (in Kelvin) and horizontal section at the first SUBMESO model level (z = 7.5m), with the horizontal wind velocity (m/s) vector and the cost line, with black line corresponds to coast line, (a) at 22.0 UTC, (b) at 24.0 UTC.
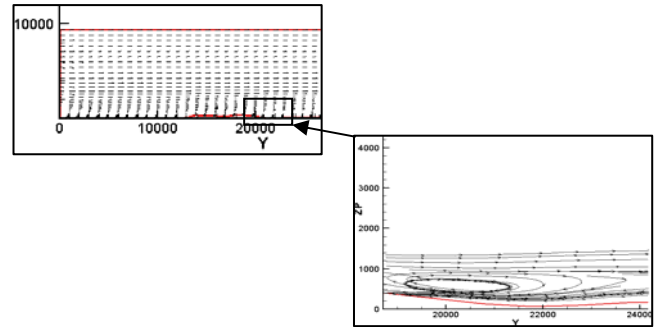

Fig. 12 The topography line with the velocity stream lines on the vertical plane (Y, Z).

CONCLUSION

The Large Eddy Simulation can be a very effective solution in the study of atmospheric flow and can carried out to the understanding of the dynamics flow phenomena even on larger scale, the ability of LES to give modeling and describe the details of thermal and dynamic parameters in an instantaneous form helped to more understand, predict and capture the flow behavior even in complex geometry.

In this study the behavior of the sea breeze been determined for the day of June 24, 2010, after the analysis of the dynamics of the atmosphere in the agglomeration of Oran, the analysis carried out to predict interval exact time of outbreak of the sea breeze, which was at 8.0 UTC. A strong relationship was marked between the sea breeze and the temperature gradient between the air over land and one above the sea. From the air dynamics of the day in question, it can be divided into four phases, the first phase between 00h and 06h, characterized by a dominant synoptic wind over the domain of a south-westerly to the south directions and a low potential temperature gradient, this gradient is insufficient to create a breeze that can defeat the wind come from the south. The second phase starts at about 7.0 UTC, as the potential temperature gradient becomes important and it able to create a more intense against the stream synoptic wind, the sea breeze appear clearly 8.0 UTC with a south-easterly direction and velocity of 5m/s. The third phase between 09:00 h and 15:00 h characterized by a minor variation of wind dynamics, where the breeze remains dominant and its speed increases with 7% as the temperature difference between the sea and the land becomes more and more important, this temperature difference decreases in the final phase of a hand by the sunset and also by the mass of cold air that arrives from the sea. Based on these results, SUBMESO model coupled with the soil model SM2-U shows a great ability to detect the phenomenon of sea breeze and even recirculation and turbulent forms, and it is sensitive to the presence of ground and foresee all ground deformation.

REFERENCES

Ding, A., Wang, T., Zhao, M., Wang, T., Li, Z. (2011) Simulation of sea-landbreezes anda discussion of their implications on the transport of air pollution during a multi-day ozone episode in the Pearl River Delta of China. *Atmos. Environ.,* **38**, 6737–6750.

Griffiths, A.D. & Middleton, J.H. (2010) Simulations of separated flow over two-dimensional hills. *J. Wind Eng. Ind. Aerodyn.*, **98**, 155–160.

Anquetin, S., Guilbaud, C., Chollet, J.P (1999) Thermal valley inversion impact on the dispersion of a passive pollutant in a complex mountainous area, *Atmos. Environ.,* **33**, 3953-3959.

Anquetin, S., Chollet, J.P., Coppalle, A., Mestayer, P.G., Sini, J.F (1998), The urban atmosphere code SUBMESO, EUROTRAC 2, *Symposium 98, Garmish March:* 23-27.

Abbs, D, & Physick, W. L. (1992) Sea-breeze observations and modeling. *Austr. Meteor. Mag.,* **41**, 7-19.

Chaouat, B. & Schiestel, R. (2013) Hybrid RANS/LES simulations of the turbulent flow over periodic hills at high Reynolds number using the PITM method. *Comp.Fluids,* **84**, 279-300.

Boone, A., Calvet, J.C., Noilhan, J. (1999) Inclusion of a Third Soil Layer in a land Surface Scheme using the Force-Restore Method, *Amer. Meteorol. Soc.,* **38**, 1611-1630.

Dupont, S. & Mestayer, P.G. (2006) Parameterisation of the urban energy budget with the Submesoscale Soil Model (SM2-U). *J. Appl. Meteorol. Climatol.,* **45**, 1744-1765.

Dupont, S., Mestayer, P.G., Guillauteau, E., Berthier, E., Andrieu, H. (2006) Parameterisation of the urban water budget with the Submesoscale Soil Model (SM2-U). *J. Appl. Meteorol. Climatol.,* **45**, 624-648.

Dupont, S.; P. G. Mestayer (2004) Evaluation of the urban soil model SM2-U on the city centre of Marseille (France), *Proc. of Fifth Symposium on Urban Environment*, A.M.S., 23-27 August, Vancouver, Canada.

Damato, F., Planchon, O., & Dubreuil, V. (2003) A remote sensing study of the inland penetration of sea breeze fronts in the English Channel. *Weather*, **58**(6), 219−226.

Finkele, K., J. M. Hacker, H. Kraus, R. A. D. Byron-Scott, (1995): A complete sea-breeze circulation cell derived from aircraft observations, *Boundary-Layer Meteorol.,* **73**, 299–317.

Jiang, G. (2012) Numerical Prediction of Turbulent Flow over 3D Sinusoidal Hill Using Non-orthogonal Hexahedron Grid and AMG Method. *Proc. of International Conference on Advances in Computational Modeling and Simulation, Procedia Engineering*: **31**, 57 − 61.

Castagna, J., Yao, Y., Yao, J. (2014) Direct numerical simulation of a turbulent flow over an axisymmetric hill. *Compu. Fluids,* **95**, 116–126.

Prospathopoulos, J.M., Politis, E.S., Chaviaropoulos, P.K. (2012) Application of a 3D RANS solver on the complex hill of Bolund and assessment of the wind flow predictions. *J. Wind Eng. Ind. Aerodyn.*, **107**–**108**, 149-159.

Loureiro, J.B.R.; Alho, A.T.P.; Freire, A.P.S. (2008) The numerical computation of near-wall turbulent flow over a steep hill. *J. Wind Eng. Ind. Aerodyn.,* **96**, 540–561.

Bouchlaghem, K., Ben Mansour, F., Elouragini, S. (2007) Impact of a sea breeze event on air pollution at the Eastern Tunisian Coast. *Atmos. Res.,* **86**, 162–172.

Ma, J-M., Wang, Fu-jun, Yu, X., Liu, Z-Q. (2011) A partially-averaged Navier-Stokes model for Hill and curved duct flow. J. Hydrodyn., **23**(4), 466-475.

Wedi, N.P. & Smolarkiewicz, P.K. (2003) Extending Gal-Chen and Somerville terrain-following coordinate transformation on time-dependent curvilinear boundaries. *J. Comput. Phys.,* **193**, 1-20.

Noihlan, J. and Planton, S. (1989) A simple parameterization of land surface processes for meteorological models. *Mon. Wea. Rev.*, **117**, 536-549.

Muppa, S.K., Anandan, V.K., Kesarkar K.A., S.Vijaya Bhaskara Rao, P. Narasimha Reddy (2012) Study on deep inland penetration of sea breeze over complex terrain in the tropics. *Atmos. Res.,* **104-105**, 209-216.

Lee, S-H,, Lee, H-W,, Kim, Y-K., Jeon W-B., Choi, H-J., Kim, D-H. (2011) Impact of continuously varied SST on land-sea breezes and ozone concentration over south-western coast of Korea. *Atmos. Environ.*, **45**, 6439-6450.

Leroyer, S. (2006) simulation numérique de l'atmosphère urbaine avec le modèle Submeso : Application a la campagne CLU-ESCOMPTE sur l'agglomération de Marseille ; *doctorat theses (PhD).*

Bastin, S., Drobinski, P., Dabas, A., Delville, P., Reitebuch, O., Werner, C. (2005) Impact of the Rhoˆne and Durance valleys on sea-breeze circulation in the Marseille area. *Atmos. Res.,* **74**, 303-328.

Simpson, J. (1994) Sea breeze and local winds*: Cambridge University Press.*

Marvakou, T., Philippopoulos, K., Deligiorgi, D. (2012) The impact of sea breeze under different synoptic patterns on air pollution within Athens basin. *Sci. Total Environ.,* 433, 31-43.

Corpetti, T. and Planchon O. (2011) Front detection on satellite images based on wavelet and evidence theory: Application to the sea breeze fronts. *Remote Sens. Environ.*, **115** 306–324.

Uchida, T. and Ohya, Y. (1997) A numerical study of stably stratified flows over a two-dimensional hill -Part I. Free-slip condition on the ground. *J. Wind Eng. Ind. Aerodyn.,* **67-68**, 493-506.

Cheng W.-L. (2002) Ozone distribution in coastal central Taiwan under sea-breeze conditions. *Atmos. Environ.,* **36**, 3445–3459.

Xue, M., Droegemeier, K.K., Wong, V. (2000) The Advanced Regional Prediction System (ARPS) - Amultiscale nonhydrostatic atmospheric simulation and prediction tool. Part I: Model dynamics and verification, *Meteor. Atmos. Phys.,* **75**, 161-193.